Brownian motion model of quantization ambiguity and universality in chaotic systems

L. Kaplan
Department of Physics, Tulane University, New Orleans, Louisiana 70118, USA
(Received 1 June 2005; published 21 September 2005)

We examine spectral equilibration of quantum chaotic spectra to universal statistics in the context of the Brownian motion model. Two competing time scales, proportional and inversely proportional to the classical relaxation time, jointly govern the equilibration process. Multiplicity of quantum systems having the same semiclassical limit is not sufficient to obtain equilibration of any spectral modes in two-dimensional systems, while in three-dimensional systems equilibration for some spectral modes is possible if the classical relaxation rate is slow. Connections are made with upper bounds on semiclassical accuracy and with fidelity decay in the presence of a weak perturbation.

DOI: 10.1103/PhysRevE.72.036214 PACS number(s): 05.45.Mt, 03.65.Sq

I. INTRODUCTION

Random matrix theory (RMT) was introduced by Wigner in the 1950s as a model for describing the universal spectral behavior of complex many-body systems such as compound nuclei. It was conjectured that a typical spectrum of a complex system displays statistical properties similar to those of a Hamiltonian chosen at random from a basis-independent ensemble of random matrices in the same symmetry class. Subsequently, Dyson showed that the statistical predictions of RMT could be reproduced within a Brownian motion model, where Brownian motion of the energy levels results from a stochastic perturbation of some initial, possibly nonrandom, Hamiltonian [1]. Bohigas, Giannoni, and Schmit argued that the same universal behavior of the spectrum occurs generically even in single-particle systems, as long as the underlying classical dynamics is chaotic [2].

Wilkinson used the Brownian motion model to explain the connection between quantum chaotic systems and RMT spectra, using the "quantization ambiguity" (i.e., multiplicity of quantum systems having the same semiclassical limit) as the source of perturbation causing Brownian motion of the energy levels and eventual equilibration to RMT spectral statistics [3]. More recently, the Brownian motion approach has been extended to study the evolution of eigenstates [4] and to relate the smooth and oscillatory parts of the spectral correlation function in diffusive and ballistic chaotic systems [5].

It well known that not all spectral modes of a typical quantum chaotic spectrum obey universal statistics. It is therefore of interest in the context of the Brownian motion model to investigate which modes are equilibrated in a given dynamical system, for a given perturbation strength (such as that arising from the quantization ambiguity), as a function of the degree of chaos in the system and as a function of effective $\hbar$. Alternatively, one may ask about the size of perturbation necessary to achieve equilibration to universal statistics for a given spectral mode; this question is related to work by Zirnbauer on energy level correlations in a quantum ensemble of classically identical maps [6], as well as to the method developed by Gornyi and Mirlin for studying wave function correlations in ballistic systems by adding weak smooth disorder [7].

In the present work, we show that the Brownian motion model can be used successfully to predict the number of equilibrated spectral modes as a function of perturbation strength, chaoticity of the classical system dynamics, system dimension, and effective $\hbar$. The equilibration process is governed by two competing time scales, allowing the number of modes equilibrated to RMT either to increase or to decrease as the original system becomes more chaotic; equilibration is reduced for systems with very short or very long classical relaxation times and is maximized for systems with intermediate Lyapunov exponent. We show that in two-dimensional quantum systems no equilibration to universal behavior for any spectral modes can arise from the quantization ambiguity in the $\hbar \to 0$ limit; in three dimensions some modes may be equilibrated depending on the classical relaxation time of the underlying classical dynamics; in four dimensions and higher, equilibration to universality will occur for at least some modes, but maximal equilibration requires the classical relaxation time to be much longer than the typical ballistic time scale of the dynamics.

The paper is organized as follows. In Sec. II, we review semiclassical estimates for matrix element variance, which are required as input for the Brownian motion model. In Sec. III, we discuss several example systems used for comparison between theory and numerics, and in Sec. IV we review the Brownian motion model itself. Two competing conditions for equilibration of spectral modes are obtained in Sec. V and applied to equilibration of the nearest level spacing distribution in Sec. VI. The implications for the effect of quantization ambiguity on spectral universality are developed in Sec. VII. Finally, in Sec. VIII we demonstrate the relationship between results obtained in the Brownian motion model and recent findings on semiclassical accuracy [8] and decay of quantum fidelity [9].

II. SEMICLASSICAL CALCULATION OF MATRIX ELEMENT VARIANCE

This discussion follows [3,4,10]. Consider the matrix elements $B_{nn}=\langle \Psi_n|\hat{B}|\Psi_n\rangle$ of an operator $\hat{B}$, given the eigenstates $|\Psi_n\rangle$ of Hamiltonian $\hat{H}$. It is assumed that the operator $\hat{B}$ is "independent" of $\hat{H}$ and has a well-defined classical limit $B(q,p)$. We also assume that the phase-space average of

the corresponding classical observable vanishes, so that the matrix elements fluctuate around zero, $\overline{B_{nn}}=0$. The variance of the matrix elements at energy E is

$$\sigma_B^2(E)=\overline{B_{nn}^2}=\nu(E)^{-1}\overline{\sum_n B_{nn}^2\delta_\eta(E-E_n)}, \tag{1}$$

where $\delta_\eta(E)=(2\pi\eta^2)^{-1/2}e^{-E^2/2\eta^2}$, $\nu(E)=\overline{\Sigma_n\delta_\eta(E-E_n)}$ is the density of states, and $\overline{\cdots}$ denotes averaging over a "suitable" ensemble. One may approximate

$$\sigma_B^2(E)\approx\frac{2\sqrt{\pi}\epsilon}{\nu(E)}\overline{\left[\sum_n B_{nn}\delta_\epsilon(E-E_n)\right]^2}, \tag{2}$$

where $\epsilon=\sqrt{2}\eta$ is of the order of but smaller than the mean level spacing $\Delta=1/\nu(E)$. In the semiclassical limit, the expression in square brackets is approximated by a trace formula

$$[\cdots]\approx\frac{1}{2\pi\hbar}\,\mathrm{Im}\sum_{p,r}T_pB_pD_{p,r}e^{iS_{p,r}/\hbar-i\mu_{p,r}\pi/2}e^{-\epsilon^2r^2T_p^2/2\hbar^2}. \tag{3}$$

Here the sum is over all primitive periodic orbits p at energy E and their repetitions r, T_p is the primitive orbit period, B_p is the classical average of the observable B over the orbit, $D_{p,r}=|\det(M_{p,r}-1)|^{-1/2}$ is the square root of a classical focusing factor, $M_{p,r}$ is the monodromy matrix of the orbit, $S_{p,r}$ is the action, and $\mu_{p,r}$ is the Maslov index. Using $\overline{(\mathrm{Im}\,f)^2}=\frac{1}{2}\,\mathrm{Re}\,\overline{f^*f}$ and neglecting repetitions, one obtains the following estimate for the variance:

$$\sigma_B^2(E)\approx\frac{2}{\beta}\frac{2\sqrt{\pi}\epsilon}{\nu(E)}(2\pi\hbar)^{-2}\sum_p T_p^2|B_p|^2D_p^2e^{-\epsilon^2T_p^2/\hbar^2}, \tag{4}$$

where as usual $\beta=1,2$ characterizes the presence or absence of time reversal symmetry, respectively. Now, assuming B_p to be real and averaging over many periodic orbits of period close to T_p,

$$B_p^2=T_p^{-2}\int_0^{T_p}dt_1\int_0^{T_p}dt_2B(t_1)B(t_2)\approx\frac{1}{T_p}\int_{-T_p/2}^{T_p/2}dt\langle B(0)B(t)\rangle, \tag{5}$$

where $\langle B(0)B(t)\rangle$ is the classical average of $B(q,p)B(q(t),p(t))$ over the energy hypersurface at energy E. Making use of the classical sum rule

$$\sum_p T_pf(T_p)D_p^2e^{-\epsilon^2T_p^2/\hbar^2}\approx 2\int_0^\infty dTf(T)e^{-\epsilon^2T^2/\hbar^2}, \tag{6}$$

one finally obtains

$$\sigma_B^2(E)\approx\frac{2}{\beta}\frac{4\sqrt{\pi}\epsilon}{\nu(E)}(2\pi\hbar)^{-2}\int_0^\infty dT\int_{-T/2}^{T/2}dt\langle B(t)B(0)\rangle e^{-\epsilon^2T^2/\hbar^2}$$

$$=\frac{2}{\beta}\frac{1}{\pi\nu(E)\hbar}\int_0^\infty dt\langle B(t)B(0)\rangle f_\epsilon(t), \tag{7}$$

with $f_\epsilon(t)=1-\mathrm{erf}(2\epsilon t/\hbar)$. This may be approximated [11] as

$$\sigma_B^2(E)\approx\frac{2}{\beta}\frac{\langle B^2\rangle}{\pi\nu(E)\hbar}\int_0^\infty dtP(t)f_\epsilon(t), \tag{8}$$

where

$$P(t)=\frac{\langle B(t)B(0)\rangle}{\langle B^2\rangle} \tag{9}$$

is a classical correlation function. For a chaotic system, $P(t)$ typically decays as a sum of exponentials [11]. The long-time behavior is then governed by the smallest exponent λ, $P(t)\approx be^{-\lambda t}$, where b is a classical constant of order unity. If the long-time behavior dominates the integral, one obtains, in the limit $\epsilon\ll\lambda\hbar$,

$$\sigma_B^2(E)\approx\frac{2}{\beta}\frac{b\langle B^2\rangle}{\pi\nu(E)\hbar\lambda}=\frac{4b\langle B^2\rangle}{\beta\lambda T_H}=\frac{4b\langle B^2\rangle T_{\mathrm{decay}}}{\beta T_H}, \tag{10}$$

where $T_H=2\pi\hbar/\Delta=2\pi\hbar\nu(E)$ is the Heisenberg time, at which individual eigenstates are resolved, and $T_{\mathrm{decay}}=\lambda^{-1}$ is a classical correlation decay time. Since $\nu(E)\propto\hbar^{-d}$, the variance decays as

$$\sigma_B^2(E)\propto\hbar^{d-1}\lambda^{-1} \tag{11}$$

for small $\hbar$. This is consistent with Shnirelman's conjecture concerning the ergodicity of chaotic eigenstates. The result is independent of the smoothing function $\delta_\epsilon(E)$. In the limit of small λ, the decay time $T_{\mathrm{decay}}=\lambda^{-1}$ becomes longer than the Heisenberg time $T_H=2\pi\hbar\nu(E)$, and λ^{-1} in Eq. (11) should be replaced with $2\pi\hbar\nu(E)$. Then $\sigma_B^2(E)\propto\hbar^0$, as expected for a quantum regular system. We can interpolate between the extreme chaotic and effectively regular regimes by taking T_{decay} intermediate between the period of the shortest orbit and the Heisenberg time.

III. CLASSICALLY CHAOTIC MAPS

As an example, consider the class of maps

$$p_{k+1}=p_k-V'(q_k),$$

$$q_{k+1}=q_k+T'(p_{k+1}), \tag{12}$$

on the torus $[-\pi,\pi)\times[-\pi,\pi)$. Any such map may be thought of as arising from the periodically kicked Hamiltonian [12,13]

$$H(p,q,t)=\frac{1}{T_{\mathrm{kick}}}T(p)+V(q)\sum_{j=-\infty}^{\infty}\delta(t-jT_{\mathrm{kick}}). \tag{13}$$

The choice $T(p)=vp^2/2+K_2v\sin p$ and $V(q)=-vq^2/2-K_1v\sin q$ corresponds to a perturbed sawtooth map. Here

$$p_{k+1}=p_k+vq_k+K_1v\cos q_k,$$

$$q_{k+1}=(1+v^2)q_k+vp_k+K_1v^2\cos q_k+K_2v\cos p_{k+1}, \tag{14}$$

and linearized motion is governed by the monodromy matrix

$$M = \begin{bmatrix} 1 & v(1 - K_1 \sin q_k) \\ v(1 - K_2 \sin p_{k+1}) & 1 + v^2(1 - K_1 \sin q_k)(1 - K_2 \sin p_{k+1}) \end{bmatrix}. \tag{15}$$

In this case, strict hyperbolicity is guaranteed for $v \neq 0$, as long as $|K_1| < 1$ and $|K_2| < 1$. The parameters K_1 and K_2 introduce nonlinearity and symmetry breaking into the dynamics. The classical Lyapunov exponent and correlation decay time T_{decay} may easily be controlled by adjusting the parameter v.

In Fig. 1, the classical autocorrelation function $P(t)$ for the perturbed sawtooth map is shown for several values of the v parameter. Clearly, the long-time decay exponent λ decreases with decreasing v, and empirically we find $\lambda_v \sim v^{3.1}$ for $v \ll 1$. Note that the correlation decay rate λ behaves very differently from the Lyapunov exponent, which scales linearly with v.

When a discrete-time map is quantized on an N-dimensional Hilbert space, we have $\hbar = 2\pi/N$, $\nu(E) = (N/2\pi)^2 T_{\text{kick}}$, and $T_H = NT_{\text{kick}}$. Then Eq. (8) becomes

$$\sigma_B^2(E) \approx \frac{2}{\beta} \frac{2\langle B^2 \rangle}{N} \left[\frac{1}{2} + \sum_{k=1}^{\infty} P(k) f_\epsilon(k) \right], \tag{16}$$

and Eq. (10) takes the form

$$\sigma_B^2(E) \approx \frac{2}{\beta} \frac{2b\langle B^2 \rangle}{\lambda N T_{\text{kick}}}. \tag{17}$$

We may also consider a system with power-law decay of classical correlations–e.g.,

$$T(p) = \frac{1}{2} p^2 + \cos(2\pi p),$$

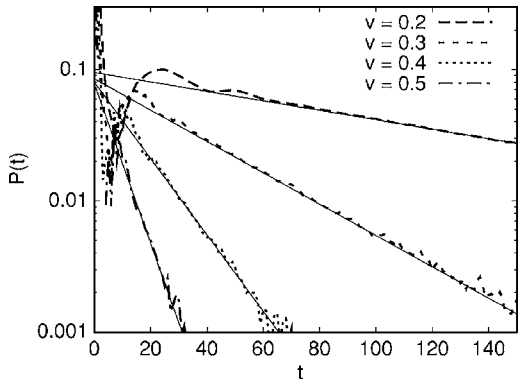

FIG. 1. The classical autocorrelation function $P(t)$ of Eq. (9) is plotted for the perturbed sawtooth map of Eq. (14), with $K_1 = 0.3$, $K_2 = -0.2$, and several values of v. $P(t)$ is computed for each of the six observables $B(q,p) = \cos(2m\pi q), \sin(2m\pi q)$, where $m = 1, 2, 3$, and then averaged to obtain the behavior for a typical observable. The thin solid lines represent best fits to the long-time exponential behavior $P(t) = be^{-\lambda_v t}$, with $\lambda_{0.2} = 0.0083$, $\lambda_{0.3} = 0.0275$, $\lambda_{0.4} = 0.067$, and $\lambda_{0.5} = 0.14$.

$$V(q) = \begin{cases} -\frac{1}{2}[q^2 - \pi^2/4] & \text{for } |q| < \pi/2, \\ 0 & \text{otherwise.} \end{cases} \tag{18}$$

Here, bouncing-ball modes for $|q| < \pi/2$ in the vicinity of $p = 0$ dominate the long-time classical correlation decay, resulting in $P(k) \sim bk^{-\gamma}$, with $\gamma = 1/3$. The sum over time steps k in Eq. (16) is effectively truncated on the scale of the Heisenberg time N by the smoothing function $f_\epsilon(k)$. Then $\Sigma_{k=1}^{N/2} P(k) f_\epsilon(k) \sim N^{2/3}$ and thus

$$\sigma_B^2(E) \sim \frac{\langle B^2 \rangle}{N^{1/3}}. \tag{19}$$

IV. BROWNIAN MOTION MODEL FOR CHAOTIC ENERGY LEVELS

The statistical properties of the energy levels E_n can be obtained using a Brownian motion model [1]. The discussion in this section follows [3–5]. In this model, the matrix elements of the Hamiltonian undergo a diffusive evolution as a function of a fictitious time variable τ. We denote the infinitesimal change of $\hat{H}$ by $\delta\hat{H}$. The off-diagonal elements of $\delta\hat{H}$ are assumed to satisfy

$$\overline{\delta H_{mn}} = 0, \quad \overline{\delta H_{mn} \delta H^*_{m'n'}} = \delta\tau C^{\text{off}}_{mn} \delta_{nn'} \delta_{mm'}, \tag{20}$$

while the diagonal elements are taken to obey

$$\overline{\delta H_{nn}} = 0, \quad \overline{\delta H_{mm} \delta H_{nn}} = \frac{2}{\beta} \delta\tau C^{\text{diag}}_{mn}. \tag{21}$$

Within RMT, $C^{\text{diag}}_{mn} = \delta_{mn}$ and $C^{\text{off}}_{mn} = 1$. Nonuniversal deviations from RMT are encoded in $C^{\text{diag}}_{mn} = C^{\text{diag}}_{m-n}$ and $C^{\text{off}}_{mn} = C^{\text{off}}_{m-n}$ [5]. The corresponding motion of the energy levels $E_0, \ldots, E_{N-1}$ may be analyzed as follows. Using second-order perturbation theory, one obtains

$$\delta E_n = \sum_{m \neq n} \frac{|\delta H_{mn}|^2}{E_n - E_m} + \delta H_{nn} \tag{22}$$

for the energy level shifts δE_n. Thus

$$\overline{\delta E_n} = \delta\tau \sum_{m \neq n} \frac{C^{\text{off}}_{m-n}}{E_n - E_m} \tag{23}$$

and

$$\overline{\delta E_m \delta E_n} = \frac{2}{\beta} \delta\tau C^{\text{diag}}_{m-n}. \tag{24}$$

It is convenient to express Eqs. (23) and (24) in terms of the Fourier modes of $\Delta E_n \equiv E_n - n\Delta$. We enforce periodic boundary conditions $\Delta E_N = \Delta E_0$ and define

$$a_k = \frac{1}{N}\sum_{n=0}^{N-1} \Delta E_n e^{-2\pi i k n/N}, \tag{25}$$

so that

$$\Delta E_n = \sum_{k=-N/2}^{N/2-1} a_k e^{2\pi i k n/N} = \sum_{k=0}^{N/2-1} a_k e^{2\pi i k n/N} + \text{c.c.} \tag{26}$$

Since the ΔE_n are real, $a_k = a_{-k}^*$. From Eq. (24) we have, using $\delta\Delta E_n = \delta E_n$,

$$\overline{\delta a_k \delta a_p^*} = \overline{\delta a_k^* \delta a_p} = \frac{2}{\beta}\delta\tau I_k \delta_{kp}, \tag{27}$$

where $I_k = N^{-1}\Sigma_n C_n^{\text{diag}} e^{2\pi i k n/N}$ and

$$\overline{\delta a_k \delta a_p} = \overline{\delta a_k^* \delta a_p^*} = 0 \tag{28}$$

for $k,p \in (0,N/2)$. In general, the expectation value of δa_k is a complicated function of all a_p, which may be expanded as

$$\overline{\delta a_k} = \delta\tau\Big(A_1(k)a_k + \sum_q A_2(k,q)a_{k-q}a_q + \sum_{q,p} A_3(k,q,p)a_q a_p a_{k-q-p} + \cdots\Big). \tag{29}$$

The coefficients A_j are obtained as follows (assuming that $C_{m-n}^{\text{off}} = 1$; see, however, Ref. [14]). Expanding the denominator $E_n - E_m$ in Eq. (23) around the mean $(n-m)\Delta$,

$$\overline{\delta E_n} \approx -\delta\tau\sum_{\ell\neq 0}\frac{1}{\ell\Delta}\Big(1 - \frac{1}{\ell\Delta}(\Delta E_{n+\ell} - \Delta E_n) + \frac{1}{2\ell^2\Delta^2}(\Delta E_{n+\ell} - \Delta E_n)^2 + \cdots\Big). \tag{30}$$

Again using $\delta E_n = \delta\Delta E_n$ and the identity $(1/N)\Sigma_n e^{-2\pi i k n/N} = \Sigma_j \delta_{k,jN}$, the first term in Eq. (30) implies

$$\overline{\delta a_k} = \delta\tau a_k \sum_{\ell\neq 0}\Big(\frac{1}{\ell^2\Delta^2}(e^{2\pi i k\ell/N} - 1) + \cdots\Big). \tag{31}$$

In the limit of large N one has, to first order in $|k|/N$ (extending the range of summation over ℓ from $-\infty$ to ∞),

$$\sum_{\ell\neq 0}\frac{1}{\ell^2\Delta^2}(e^{2\pi i k\ell/N} - 1) \approx -\frac{2\pi^2|k|}{N\Delta^2} \tag{32}$$

and thus

$$A_1(k) = -\frac{2\pi^2|k|}{N\Delta^2}. \tag{33}$$

To lowest order in Eq. (29), the equilibrium distribution of the a_k (corresponding to large fictitious time τ) factorizes into a product of Gaussians, where the variance is given by

$$\overline{|a_k|^2} = \frac{2}{\beta}\frac{N\Delta^2 I_k}{4\pi^2 k}, \tag{34}$$

while higher-order cumulants are zero. The approximation of Eq. (34) is appropriate for $k \ll N$. In this case, the a_k for different k are uncorrelated. In RMT, $I_k = N^{-1}$ and

$$\overline{|a_k|^2} = \frac{2}{\beta}\frac{\Delta^2}{4\pi^2 k} \tag{35}$$

for $k \ll N$.

In order to determine the fluctuations of a_k for $k \sim N$, higher-order terms in Eq. (29) must be taken into account. This may be done perturbatively, resulting in corrections to the variance and possibly nonzero higher-order cumulants. Moreover, a_k for larger values of k may be correlated.

In the above derivation, we have started with initial conditions $a_k = 0$ at fictitious time $\tau = 0$, i.e., we have assumed that the initial unperturbed Hamiltonian has a "picket fence" spectrum, $E_n = n\Delta$. A typical chaotic Hamiltonian, however, will not correspond naturally to a small perturbation of such a "picket fence" Hamiltonian. Therefore, in practice it is more useful to observe spectral equilibration by comparing coefficients a_k of a given Hamiltonian $\hat{H}$ with the coefficients a_k' of a perturbed Hamiltonian $\hat{H} + \hat{B}$. Full equilibration implies that the spectra of $\hat{H}$ and $\hat{H} + \hat{B}$ become independent of one another, though drawn from the same random matrix ensemble. Then

$$\overline{|a_k - a_k'|^2} = \frac{2}{\beta}\frac{\Delta^2}{2\pi^2 k} = \frac{C_\beta}{k} \tag{36}$$

for $k \ll N$.

V. CONDITIONS FOR ENERGY LEVEL EQUILIBRATION

We now address more carefully the question originally raised in the seminal work by Wilkinson [3]. Specifically, we wish to understand under what circumstances a class of classically small perturbations $\hat{B}$ of an initial Hamiltonian $\hat{H}$ is sufficient to generate random matrix statistics in the spectrum, at various energy scales. A related question is the size in parameter space of a random chaotic ensemble necessary to average away system-specific spectral properties and generate universal statistics [6,7].

Two conditions are necessary for equilibration to universal statistics to occur. First, if the perturbation is classically small, then equilibration to RMT may only occur on time scales longer than the decay time of classical correlations (otherwise, $I_k \neq N^{-1}$ for the corresponding modes a_k). Thus, the modes a_k may be equilibrated to RMT only for $k \gg T_{\text{decay}}/T_{\text{kick}}$, independent of the perturbation, and correspondingly the spectrum may only display universal statistics on energy scales $\mathcal{E} \ll \hbar/T_{\text{decay}}$. Second, the perturbation must be sufficiently strong to equilibrate a given mode a_k after the fictitious time τ during which the Hamiltonian matrix elements undergo Brownian motion. In our units, this fictitious time τ is simply equal to the variance [3],

$$\tau = \sigma_B^2, \tag{37}$$

and is given by Eq. (10). On the other hand, the characteristic response time of the kth mode is

$$\tau_k = \frac{\hbar}{\pi\nu(E)(kT_{\rm kick})} = \frac{2\hbar^2}{(kT_{\rm kick})T_H}, \tag{38}$$

as may easily be seen by comparing Eqs. (27) and (34) and then noting that the Heisenberg time T_H is given by $2\pi\hbar/\Delta = 2\pi\hbar\nu(E) = NT_{\rm kick}$. Equilibration will therefore happen for a given mode a_k when $\tau \gg \tau_k$, i.e.,

$$k \gg \frac{\hbar^2}{\langle B^2\rangle T_{\rm decay} T_{\rm kick}}, \tag{39}$$

and transforming to the energy domain we find equilibration on scales

$$\mathcal{E} \ll \frac{\langle B^2\rangle T_{\rm decay}}{\hbar}. \tag{40}$$

The condition of Eq. (40) must be satisfied simultaneously with the first condition $\mathcal{E} \ll \hbar/T_{\rm decay}$; i.e., equilibration to universal statistics occurs on all energy scales $\mathcal{E}$ satisfying

$$\mathcal{E} \ll \mathcal{E}_{\rm equil} \sim \min\left(\frac{\hbar}{T_{\rm decay}}, \frac{\langle B^2\rangle T_{\rm decay}}{\hbar}\right). \tag{41}$$

Note that the two upper limits on the equilibration energy scale have opposite dependence on the classical correlation scale $T_{\rm decay}$.

Let us consider the behavior of the system as the size of the perturbation $\hat{B}$ is varied, for a given initial Hamiltonian $\hat{H}$, at a given classical energy. We assume $T_{\rm decay} < T_H$, so that the system is in the quantum chaotic regime. (i) For very small perturbations, $\langle B^2\rangle \ll \hbar^2/(T_{\rm decay}T_H)$, there is no equilibration on any time scale before the Heisenberg time T_H and consequently no equilibration on any energy scale larger than a mean level spacing Δ. (ii) For larger perturbations—i.e., $\hbar^2/(T_{\rm decay}T_H) \ll \langle B^2\rangle \ll \hbar^2/T_{\rm decay}^2$—all modes $k \gg k_{\rm min} \sim \hbar^2/(T_{\rm kick}T_{\rm decay}\langle B^2\rangle)$ equilibrate to their RMT values. In the energy domain, the corresponding condition is $\mathcal{E} \ll \mathcal{E}_{\rm equil} \sim \langle B^2\rangle T_{\rm decay}/\hbar$. (iii) Finally, for the largest (still classically small) perturbations $\hbar^2/T_{\rm decay}^2 \ll \langle B^2\rangle \ll E^2$, all time scales beyond $T_{\rm decay}$ and all energy scales below $\mathcal{E}_{\rm equil} \sim \hbar/T_{\rm decay}$ equilibrate to universal statistics.

What happens if we instead fix the size of perturbation $\hat{B}$ and consider a variety of classical systems with different classical time scales $T_{\rm decay}$? (i) For the most strongly chaotic systems, $T_{\rm decay} \ll \hbar\langle B^2\rangle^{-1/2}$, and equilibration is limited by the condition of Eq. (40). (ii) As the classical system becomes less chaotic, $k_{\rm min}$ falls, more and more modes a_k come into equilibrium, and the energy scale $\mathcal{E}_{\rm equil}$ increases. (iii) Maximum equilibration to RMT is attained when $T_{\rm decay} \sim \hbar\langle B^2\rangle^{-1/2}$, where all modes a_k for $k > k_{\rm min} \sim \hbar T_{\rm kick}^{-1}\langle B^2\rangle^{-1/2}$ equilibrate and $\mathcal{E}_{\rm equil} \sim \langle B^2\rangle^{1/2}$. (iv) Then, as the degree of chaoticity of the system continues to decrease, $k_{\rm min}$ begins to increase, modes again move away from RMT equilibrium, and the energy $\mathcal{E}_{\rm equil}$ begins to drop. (v) Eventually, we reach the border $T_{\rm decay} \sim T_H$ between quantum chaos and quantum regularity, where all equilibration to universal statistics is again absent. Thus, the absence of equilibration to RMT at a given time or energy scale may be consistent with either very strongly chaotic or very weakly chaotic (or regular) systems, while maximum possible equilibration is attained for moderately chaotic systems between these two extremes.

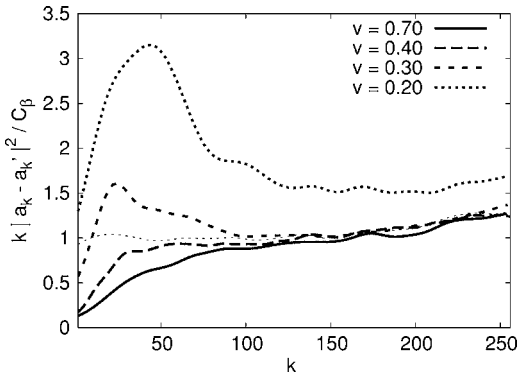

FIG. 2. The effect of a perturbation on the quantum spectrum as a function of Fourier mode k is plotted for four classical systems, distinguished by the parameter v of Eq. (14). The values of K_1 and K_2 are as in Fig. 1, and the Hilbert space dimension is $N=512$. As in the previous figure, the data are averaged over an ensemble of perturbations $B(q,p) = \Sigma_{m=1}^{3}[x_m \sin(2\pi mq) + y_m \cos(2\pi mq)]$ with $\langle B^2\rangle = \frac{1}{2}\Sigma_{m=1}^{3}(x_m^2 + y_m^2) = 0.6N^{-3} = 4.51\times 10^{-9}$. The constant C_β, is given by Eq. (36), where $\beta=2$ in the present case. The thin dotted curve indicates the limit of full equilibration on all energy scales, as obtained by choosing random and uncorrelated Hamiltonians $\hat{H}$ and $\hat{H}' = \hat{H} + \hat{B}$.

The discussion of the preceding paragraph is illustrated for the perturbed sawtooth map in Fig. 2, where we show the effect on the spectrum at various energy scales of a fixed-size perturbation, for four classical systems characterized by different decay times $T_{\rm decay}$. The classical systems treated here are the same as in Fig. 1, while the family of perturbations used corresponds precisely to the family of classical functions used in that earlier figure. The squared change in each Fourier spectral coefficient a_k has been normalized by the constant C_β of Eq. (36), so that full equilibration implies $k|a_k - a_k'|^2/C_\beta = 1$ for $k \ll N$. For $k \sim N$, this result is modified due to higher-order terms in Eq. (29), as discussed in Sec. IV and illustrated by the thin dotted curve in Fig. 2. From $v=0.70$ to $v=0.20$, the four systems clearly demonstrate the effect of gradually reducing the Lyapunov exponent and increasing the classical parameter $T_{\rm decay}$.

Looking first at the $v=0.70$ curve in Fig. 2, we find equilibration of the spectrum only for $k \gtrsim 100$, corresponding approximately to energy scales of three levels spacings or fewer. When the degree of chaos is reduced ($v=0.40$) and $T_{\rm decay}$ correspondingly increases, the same perturbation strength is sufficient to equilibrate the spectrum up through much larger energy scales—namely, $k \gtrsim k_{\rm min} \approx 50$. However, further reducing the degree of chaos by tuning v down below 0.4 and thereby increasing $T_{\rm decay}$ serves to *reduce* the range of equilibrated energies for the same perturbation strength, as equilibration is now governed by the condition $k \gg T_{\rm decay}/T_{\rm kick}$. Finally, for $v=0.20$, $T_{\rm decay}/T_{\rm kick} = 120$, and once again equilibration to universal behavior is not attained on any energy scale for our system size.

VI. EQUILIBRATION OF LEVEL SPACINGS

In the previous section we considered spectral equilibration at various time scales $kT_{\rm kick}$ and energy scales E. We

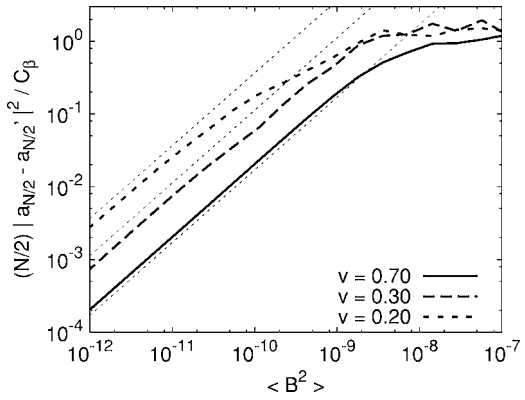

FIG. 3. Equilibration of the highest-frequency mode in the spectrum is studied for $N=256$ as a function of perturbation strength for several initial Hamiltonians. The classical systems as well as the ensemble of perturbations are the same as in Fig. 2. The thin dotted lines correspond to the classical prediction $|a_{N/2}-a'_{N/2}| \propto \langle B^2\rangle \int_0^\infty dt P(t)$.

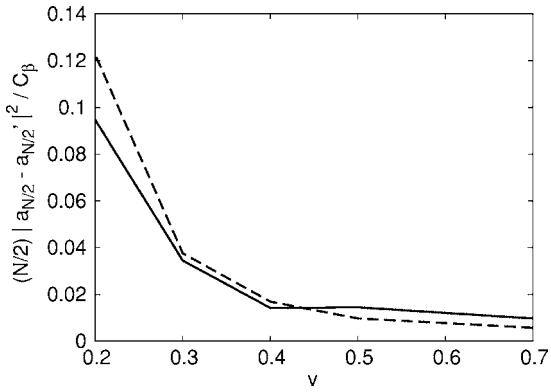

FIG. 4. Equilibration of the highest-frequency mode in the spectrum is studied for $N=1024$ and perturbation strength $\langle B^2\rangle = 6.4 \times 10^{-7}$ as a function of the classical parameter v (solid curve). The classical systems and the ensemble of perturbations are the same as in Figs. 2 and 3. The classical prediction based on Eq. (8) is indicated by the dashed curve.

now focus specifically on the conditions for equilibration at the energy scale Δ, necessary, for example, to reproduce the Wigner-Dyson distribution of nearest-neighbor level spacings. Assuming $T_{\text{decay}} < T_H$ as before, we need to satisfy Eq. (40) for $\mathcal{E} \sim \Delta$:

$$\langle B^2\rangle \gg \frac{\hbar\Delta}{T_{\text{decay}}} \propto \frac{\hbar^{d+1}}{T_{\text{decay}}}. \tag{42}$$

The size of the perturbation $\hat{B}$ must generically be at least of order $\hbar^{(d+1)/2}$ to produce equilibration of the level spacings. Less chaotic systems, however, as measured by a longer decay time, equilibrate more efficiently. For example, in a two-dimensional Hamiltonian system, $B \propto \hbar^{3/2}$ is needed for a fixed T_{decay}, but $B \propto \hbar^{7/4}$ would be sufficient if $T_{\text{decay}} \propto T_H^{1/2}$ and $B \propto \hbar^{2-\epsilon/2}$ suffices if $T_{\text{decay}} \propto T_H^{1-\epsilon}$.

Equilibration at the scale of the mean level spacing may be measured by focusing on the Fourier coefficient $a_{N/2}$ (notice that $a_N = a_0$). Equilibration of this coefficient is studied in Fig. 3 as a function of perturbation strength for several classical Hamiltonians. Specifically, the mean-squared fluctuation in the $a_{N/2}$ coefficient is plotted as a function of perturbation strength $\langle B^2\rangle$. For each classical system, we clearly observe the proportionality between $|a_{N/2}-a'_{N/2}|^2$ and $\langle B^2\rangle$ when $|a_{N/2}-a'_{N/2}|^2 \ll N^{-1}$ and the eventual saturation at the system-independent equilibrium value at large perturbation size, just as predicted by the Brownian motion model. Furthermore, at a given perturbation strength, we see faster equilibration for systems with slower classical correlation falloff, as indicated by the smaller classical parameter v. Semiclassically, we expect this increase in equilibration rate to be controlled by the integral $\int_0^\infty dt P(t) \approx b T_{\text{decay}}$ as in Eqs. (8) and (10); the classical predictions are indicated by dotted lines in Fig. 3. The slight discrepancy between the quantum data and the semiclassical prefactors may be explained by the finite system size $N=256$, since the classical expressions assume $N \gg T_{\text{decay}}/T_{\text{kick}}$, while in our case $N=256$ and $T_{\text{decay}}/T_{\text{kick}}$ reaches 120 when $v=0.2$.

Figure 4 shows explicitly the dependence of equilibration rate on the classical system dynamics by varying the classical parameter v while the perturbation strength is held fixed. Again, we see an order-of-magnitude change in the equilibration rate as v is varied, in agreement with the semiclassical prediction indicated by the dashed curve.

VII. QUANTIZATION AMBIGUITY AND SPECTRAL EQUILIBRATION

The original motivation behind Wilkinson's work [3] was to understand the relationship between spectral equilibration and the quantization ambiguity, thus using the latter to explain the approach of generic chaotic systems to RMT behavior on short energy scales. Generally, quantization ambiguities come in two types. The first are gauge or boundary condition ambiguities that allow many different semiclassical theories to be associated with the same classical dynamics, as in the Aharonov-Bohm effect or in a change from Dirichlet to Neumann boundary conditions for a billiard system. These ambiguities correspond to $O(\hbar_{\text{eff}})$ terms in the quantum Hamiltonian, where $\hbar_{\text{eff}} = \hbar/S_{\text{typ}} \sim \hbar/ET_{\text{kick}} \sim \hbar/pL$, S_{typ} is the typical action of a short classical orbit, p is the typical momentum, and L is the system size. Second, there are operator ordering ambiguities that allow multiple quantum Hamiltonians to have the same semiclassical limit, including identical action phases at leading order. Ambiguities of this second class are $O(\hbar_{\text{eff}}^2)$ and result, for example, from canonically quantizing the same classical Hamiltonian in two coordinate systems related by a nonlinear canonical transformation [3]; they also appear naturally when different limiting procedures are used to define a quantum dynamics on a constrained surface [15].

We first examine spectral equilibration due to the $O(\hbar_{\text{eff}}^2)$ quantization ambiguity, considered by Wilkinson in Ref. [3]. Substituting $B \sim \hbar_{\text{eff}}^2 E$ into Eq. (41), we find equilibration on energy scales

$$\mathcal{E} \ll \mathcal{E}_{\text{equil}} = E \min\left(\hbar_{\text{eff}} \frac{T_{\text{kick}}}{T_{\text{decay}}}, \hbar_{\text{eff}}^3 \frac{T_{\text{decay}}}{T_{\text{kick}}}\right) \tag{43}$$

or, equivalently, for Fourier modes

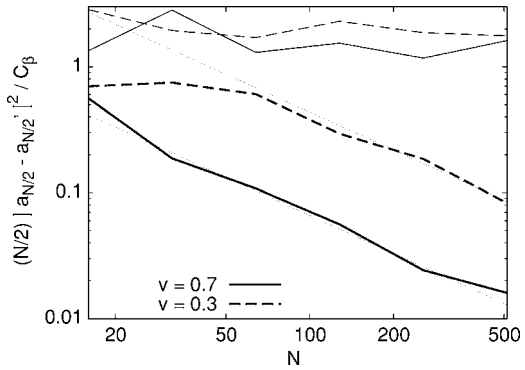

FIG. 5. Equilibration of the highest-frequency mode in the spectrum of a perturbed sawtooth map is shown for $O(\hbar_{\rm eff}^2)$ perturbation strength $\langle B^2\rangle=(0.66/N^2)^2$ (thick curves) and $O(\hbar_{\rm eff})$ perturbation strength $\langle B^2\rangle=(0.16/N)^2$ (thin curves) as a function of N. The thin dotted lines indicate the predicted N^{-1} behavior for the $O(\hbar_{\rm eff}^2)$ case in the semiclassical limit $N\to\infty$.

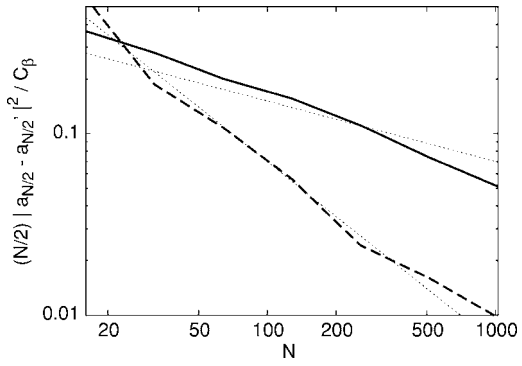

FIG. 6. Equilibration of the highest-frequency mode in the spectrum is shown for $O(\hbar^2)$ perturbation strength $\langle B^2\rangle=(0.66/N^2)^2$ for a system with power-law classical correlation decay, defined by Eq. (18), solid curve, and for the perturbed sawtooth map with $v=0.7$, dashed curve. The thin dotted lines indicate the predicted $N^{-\gamma}$ behavior for $\gamma=1/3$ and $\gamma=1$.

$$k \gg k_{\rm min} = \max\left(\frac{T_{\rm decay}}{T_{\rm kick}}, \hbar_{\rm eff}^{-2}\frac{T_{\rm kick}}{T_{\rm decay}}\right). \tag{44}$$

For a fixed classical dynamics, the second expression in the parentheses in Eq. (43) or (44) always dominates in the semiclassical limit $\hbar_{\rm eff}\to 0$. For a d-dimensional Hamiltonian system, the total number of available fluctuating modes in the spectrum is $O(\hbar_{\rm eff}^{1-d})$, and all but the first $O(\hbar_{\rm eff}^{-2}T_{\rm kick}/T_{\rm decay})$ of these are equilibrated. Thus, full equilibration is not possible for any spectral mode in the case $d=2$, while for $d=3$ full equilibration is possible for the highest-k modes, assuming slow decay of classical correlations, $T_{\rm decay}/T_{\rm kick}\gg 1$. In the energy domain, this implies equilibration only on scales up to $O(T_{\rm decay}/T_{\rm kick})$ mean level spacings Δ in the three-dimensional case. The case $d=4$ (e.g., two interacting particles in two dimensions) is the first for which equilibration generically extends to scales much larger than a mean level spacing, $\mathcal{E}_{\rm equil}\gg\Delta$. Finally, in the many-body limit $d\to\infty$, an ever-increasing number of modes are equilibrated by the $O(\hbar_{\rm eff}^2)$ ambiguity; however, the first $O(\hbar_{\rm eff}^{-2}T_{\rm kick}/T_{\rm decay})$ modes are never equilibrated. Correspondingly the range of energies over which equilibration may occur always remains a factor of $O(\hbar_{\rm eff}^2 T_{\rm decay}/T_{\rm kick})$ smaller than the ballistic Thouless energy $E_{\rm Thouless}\sim\hbar_{\rm eff}E$, independent of dimension.

We now turn to the $O(\hbar_{\rm eff}^{-1})$ quantization ambiguity, associated with external gauge fields or boundary conditions. A similar analysis shows that equilibration now occurs on energy scales $\mathcal{E}\ll\mathcal{E}_{\rm equil}\sim\hbar_{\rm eff}ET_{\rm kick}/T_{\rm decay}$ and for Fourier modes $k\gg k_{\rm min}\sim T_{\rm decay}/T_{\rm kick}$. Thus, all modes equilibrate in any dimension for a chaotic system, except for the first few that encode nonuniversal short-time dynamics for a classical system with slow correlation decay.

In Fig. 5, we again focus on equilibration of the highest-frequency Fourier mode $a_{N/2}$, corresponding to energy scales of order Δ, for our quantum map numerical model (which exhibits the scaling of a $d=2$ autonomous Hamiltonian system). Consistently with the above discussion, an $O(\hbar_{\rm eff}^2)$ ambiguity is not sufficient to equilibrate even this highest-frequency Fourier mode in the semiclassical limit $N\to\infty(\hbar_{\rm eff}\to 0)$; lower-frequency modes will be even further away from equilibration. On the other hand, an $O(\hbar_{\rm eff})$ (gauge-size) ambiguity provides full equilibration independent of $\hbar_{\rm eff}$.

The above analysis and numerical simulation assume a constant $T_{\rm decay}$ in the $\hbar_{\rm eff}\to 0$ limit. However, a system remains in the quantum chaotic regime as long as $T_{\rm decay}$ is shorter than the Heisenberg time—i.e., when $T_{\rm decay}/T_{\rm kick}<\hbar_{\rm eff}^{1-d}$. In general, the rate of equilibration to RMT behavior is increased by choosing a system with very slow classical relaxation, $T_{\rm decay}\gg T_{\rm kick}$. For the $d=2$ case, it is impossible to attain complete equilibration to RMT for any spectral mode with an $O(\hbar_{\rm eff}^2)$ perturbation, regardless of the choice of classical system. For $d\geqslant 3$, on the other hand, Eqs. (43) and (44) clearly indicate that full equilibration for some modes can be achieved with an $O(\hbar_{\rm eff}^2)$ perturbation for systems with $T_{\rm decay}/T_{\rm kick}\gg 1$ (where a generic chaotic system with $T_{\rm decay}/T_{\rm kick}\sim 1$ would not display equilibrated behavior). Optimal equilibration is attained for $T_{\rm decay}/T_{\rm kick}\sim\hbar_{\rm eff}^{-1}$, where all but the lowest $O(\hbar_{\rm eff}^{-1})$ modes are equilibrated in any dimension $d\geqslant 3$.

Finally, in Fig. 6 we compare equilibration in the hard chaotic perturbed sawtooth map with equilibration in a system governed by a slow power-law classical decay, defined by Eq. (18). In both cases a perturbation of order $\hbar_{\rm eff}^2\sim N^{-2}$ is used. Although no equilibration is possible for any system in $d=2$, we see clearly that the power-law classical system comes closer to equilibration than the hard chaotic system for any large N, and the two systems are governed by different exponents in the $N\to\infty$ limit.

VIII. FIDELITY AND SEMICLASSICAL ACCURACY

The fidelity of quantum evolution in the presence of a small perturbation, also known as the Loschmidt echo, has received much attention recently, particularly in the context of classical-quantum correspondence and the very different behaviors that the quantum fidelity can exhibit for classically regular and chaotic systems [16]. For sufficiently large per-

turbations, the decay of quantum fidelity with time can be governed by the classical Lyapunov exponent [17,18]. Here we wish to mention an interesting connection between spectral equilibration and fidelity decay in quantum chaotic systems due to a *small* perturbation, as analyzed recently by Prosen and collaborators [9]. It was shown that for a static perturbation $\hat{B}$ with $\langle B^2\rangle < \hbar^2/T_{\mathrm{decay}}^2$, the fidelity decays exponentially on a time scale varying inversely with T_{decay}—namely, $T_{\mathrm{fidelity}} \sim \hbar^2/\langle B^2\rangle T_{\mathrm{decay}}$. Dividing through by the one-step time scale T_{kick}, we find that T_{fidelity} corresponds to a dimensionless mode number

$$k_{\mathrm{fidelity}} \sim \frac{\hbar^2}{\langle B^2\rangle T_{\mathrm{decay}} T_{\mathrm{kick}}}, \tag{45}$$

which precisely agrees with the boundary between equilibrated and nonequilibrated modes given by Eq. (39), valid as long as $k_{\mathrm{fidelity}} > T_{\mathrm{decay}}/T_{\mathrm{kick}}$. In other words, a mode k is equilibrated to universal behavior by a given class of perturbations if and only if two conditions hold simultaneously: the quantum fidelity has decayed to a value much less than unity by the corresponding time kT_{kick} *and* this time scale kT_{kick} is larger than the classical relaxation time T_{decay}.

Another important connection is between spectral equilibration behavior discussed in the present work and the decay of semiclassical accuracy. Since different quantizations of the same semiclassical dynamics differ by $O(\hbar_{\mathrm{eff}}^2)$ in the Hamiltonian, the difference between a typical quantization and the semiclassical approximation must be at least of this order in the $\hbar_{\mathrm{eff}} \to 0$ limit. Thus the error in the semiclassical approximation must be at least of the same size as the error caused by an $O(\hbar_{\mathrm{eff}}^2)$ perturbation in quantum mechanics, assuming of course that the physically correct quantization is "typical." Clearly, hard quantum effects such as diffraction can increase the error in the semiclassical approximation, so the $O(\hbar_{\mathrm{eff}}^2)$ quantization ambiguity only provides a lower bound on the size of the semiclassical error or, equivalently, an upper bound on the breakdown time of semiclassical validity. Previous work has shown that this bound on the semiclassical error is saturated for the case of a smooth Hamiltonian in the absence of caustics [8], and furthermore it was demonstrated that the semiclassical error obeys different scaling laws with time and $\hbar$ for regular as opposed to chaotic classical systems, just as one would predict using the quantization ambiguity approach. The semiclassical accuracy problem may also be considered as an example of a generalized quantum fidelity problem, if non-Hermitian perturbations are considered (since semiclassical evolution is in general nonunitary).

The results of the present work, particularly those of Sec. VII imply an upper bound on the breakdown time scale of semiclassical accuracy, $T_{\mathrm{semiclassical}} \sim \hbar_{\mathrm{eff}}^{-2} T_{\mathrm{kick}}^2/T_{\mathrm{decay}}$, and a lower bound on the breakdown energy scale of semiclassical accuracy,

$$\mathcal{E}_{\mathrm{semiclassical}} \sim E\hbar_{\mathrm{eff}}^3 \frac{T_{\mathrm{decay}}}{T_{\mathrm{kick}}} \sim E_{\mathrm{Thouless}} \hbar_{\mathrm{eff}}^2 \frac{T_{\mathrm{decay}}}{T_{\mathrm{kick}}}, \tag{46}$$

where E_{Thouless} is a ballistic Thouless energy. In particular, semiclassical accuracy will persist beyond the Heisenberg time $T_H \sim \hbar_{\mathrm{eff}}^{-1} T_{\mathrm{kick}}$ in any two-dimensional chaotic system (assuming diffraction and caustics are properly accounted for), allowing individual energy levels and wave functions to be semiclassically resolved. In three-dimensional systems, $T_H \sim \hbar_{\mathrm{eff}}^{-2} T_{\mathrm{kick}}$ and $T_{\mathrm{semiclassical}} \sim T_H T_{\mathrm{kick}}/T_{\mathrm{decay}}$. Here, the semiclassical breakdown time may be comparable to the Heisenberg time for the most chaotic systems ($T_{\mathrm{decay}}/T_{\mathrm{kick}} \sim 1$), but any slowdown in the classical relaxation rate will cause a faster breakdown in the semiclassical approximation. Finally, given four or more classical degrees of freedom, semiclassical accuracy inevitably breaks down well before the Heisenberg time for any generic dynamics, even the most chaotic, and semiclassical reproduction of individual spectral levels is never possible. It may be of interest to investigate the manner in which improved semiclassical approximations beyond leading order in $\hbar$ [19] may produce different scaling of the semiclassical error and possibly permit quantum spectra to be semiclassically resolved in four dimensions and higher.

IX. SUMMARY

A careful examination of the Brownian motion model for spectral equilibration to universal statistics shows that equilibration is strongly dependent on the classical relaxation rate as well as on the dimensionality of the system. Two competing time scales, proportional and inversely proportional to the classical relaxation time T_{decay}, jointly govern the equilibration process. Balancing of these two time scales implies that for a given perturbation B, equilibration of the maximum number of spectral modes is achieved when $T_{\mathrm{decay}} \sim \hbar\langle B^2\rangle^{-1/2}$. For small perturbations $B < \hbar/T_{\mathrm{decay}}$, a relation exists between spectral equilibration as a function of mode number k and the decay of the quantum fidelity as a function of time.

Focusing on the effect of $O(\hbar_{\mathrm{eff}}^2)$ perturbations, associated with the ambiguity of quantization, we find that no equilibration to universal statistics is ever possible for dynamics in two dimensions. In three dimensions, equilibration to universal statistics occurs for some modes, but only if the classical relaxation time T_{decay} is sufficiently long, while in four dimensions and higher, equilibration of at least some modes occurs for any chaotic system. However, optimal equilibration only occurs for very long classical relaxation times $T_{\mathrm{decay}} \propto \hbar_{\mathrm{eff}}^{-1}$. These predictions of the Brownian motion model are also entirely consistent with results for semiclassical accuracy in smooth chaotic systems.

ACKNOWLEDGMENTS

The author is grateful to B. Mehlig for invaluable contributions in the early stages of this work and to M. Wilkinson and U. Smilansky for very useful discussions. This work was supported in part by the U.S. Department of Energy Grant No. DE-FG03-00ER41132 and Louisiana Board of Regents Support Fund Contract No. LEQSF(2004-07)-RD-A-29.

[1] F. J. Dyson, J. Math. Phys. **3**, 1191 (1962); **13**, 90 (1972).
[2] O. Bohigas, M.-J. Giannoni, and C. Schmit, J. Phys. (France) Lett. **45**, L-1015 (1984).
[3] M. Wilkinson, J. Phys. A **21**, 1173 (1988).
[4] M. Wilkinson and P. N. Walker, J. Phys. A **28**, 6143 (1996).
[5] B. Mehlig and M. Wilkinson, Phys. Rev. E **63**, 045203(R) (2001).
[6] M. R. Zirnbauer, in *Supersymmetry and Trace Formulae: Chaos and Disorder*, edited by I. V. Lerner, J. P. Keating, and D. E. Khmelnitskii (Plenum, New York, 1999).
[7] I. V. Gornyi and A. D. Mirlin, Phys. Rev. E **65**, 025202(R) (2002); J. Low Temp. Phys. **126**, 1339 (2002).
[8] L. Kaplan, Phys. Rev. E **70**, 026223 (2004); **58**, 2983 (1998).
[9] T. Prosen and M. Znidaric, J. Phys. A **35**, 1455 (2002); T. Prosen and T. H. Seligman, *ibid.* **35**, 4707 (2002).
[10] B. Eckhardt, S. Fishman, J. Keating, O. Agam, J. Main, and K. Müller, Phys. Rev. E **52**, 5893 (1995).
[11] R. Artuso and A. Prampolini, Phys. Lett. A **246**, 407 (1998); R. Artuso, Physica D **131**, 68 (1999).
[12] S. Fishman, D. R. Grempel, and R. E. Prange, Phys. Rev. Lett. **49**, 509 (1984).
[13] G. Casati, B. V. Chirikov, F. M. Izraelev, and J. Ford, in *Stochastic Behavior in Classical and Quantum Hamiltonian Systems*, edited by G. Casati and J. Ford, *Lecture Notes in Physics*, Vol. 93 (Springer, Berlin, 1979).
[14] J. T. Chalker, I. V. Lerner, and R. A. Smith, Phys. Rev. Lett. **77**, 554 (1996).
[15] K. A. Mitchell, Phys. Rev. A **63**, 042112 (2001); P. Maraner, J. Phys. A **28**, 2939 (1995).
[16] J. Emerson, Y. S. Weinstein, S. Lloyd, and D. G. Cory, Phys. Rev. Lett. **89**, 284102 (2002).
[17] R. A. Jalabert and H. M. Pastawski, Phys. Rev. Lett. **86**, 2490 (2001).
[18] P. Jacquod, P. G. Silvestrov, and C. W. J. Beenakker, Phys. Rev. E **64**, 055203(R) (2001).
[19] K. Weibert, J. Main, and G. Wunner, Eur. Phys. J. D **19**, 379 (2002).